A compact cascaded microring filter with two master rings and two slave rings for sensing application*

ZHANG Xin (张鑫)**, **LI Zhi-quan** (李志全), **and TONG Kai** (童凯)
College of Electrical Engineering, Yanshan University, Qinhuangdao 066004, China

(Received 27 September 2013)

In this paper, an ultra compact cascaded microring filter consisting of two master rings with radius of 2.5 μm and two slave rings with radius of 1 μm is presented and studied theoretically. The filter with a very large free spectral range (FSR) of 206 nm, a deep extinction ratio of 23 dB, a high quality factor of 2.76×10^5, and greatly suppressed spurious modes of less than 0.1 dB is achieved. The spectral responses of the filter are simulated by transfer matrix method, and the results show that this filter has a great potential of sensor application.
Document code: A **Article ID:** 1673-1905(2014)01-0016-5
DOI 10.1007/s11801-014-3174-z

Microring resonators have attracted more and more attention, and many demonstrations of integrated devices, including add/drop filters[1-3], sensors[4], modulators[5], wavelength selectors[6] and signal processors[7], have been presented.

Microring filters based on silicon-on-insulator (SOI) with high quality factor (Q-factor) can be used in high sensitivity sensors[8-11]. In order to obtain higher Q-factor, it is important to minimize the intrinsic loss and choose a small coupling coefficient. Utilizing a Mach-Zehnder interferometer coupler is also a useful way to control the coupling coefficient[12]. Besides, a large free spectral range (FSR) means a large test range[13]. And the easiest way to enlarge FSR is to decrease the radius of ring[2,14]. Based on the Vernier effect, creating multi-stage structures by cascading several rings with larger radius is another useful method for FSR expansion. Feng[15] and Lu[16] both presented their configurations to double the FSR. Thus, if we can effectively suppress the spurious mode caused by the cascading of small rings, an ultra large FSR filter is possible to be realized.

In this paper, a cascaded microring resonator filter with ultra large FSR is proposed. In order to suppress the spurious mode and expand the FSR, each cascaded master ring has one slave ring embedded. According to the simulation, the structure we designed consisting of two master rings with radius of 2.5 μm and two slave embedded rings with radius of 1 μm has an ultra high Q-factor of 2.76×10^5, a quasi-FSR about 206 nm, greatly suppressed spurious modes and obvious extinctions at resonant waveguide, which performs very well as a narrow band filter to offer high resolution for high sensitivity sensing.

The schematic diagram of the cascaded microring filter with two master rings and two slave rings is shown in Fig.1. The microrings are made of SOI ridge waveguide with height of 220 nm and width of 450 nm. The radii of master rings and slave rings are 2.5 μm and 1 μm, respectively. To satisfy the guided mode around 1550 nm, the effective index of rings and waveguides is set as 3.2. The bend loss coefficient of master rings α_m is 2.5×10^{-6} μm^{-1}, and that of slave rings α_s is 5.5×10^{-6} μm^{-1}. A phase shifter is added in the end of bottom bus to ensure the light signal from bottom bus keeps the same phase with that from top bus. Therefore, the phase change error caused by the change of optical path can be eliminated.

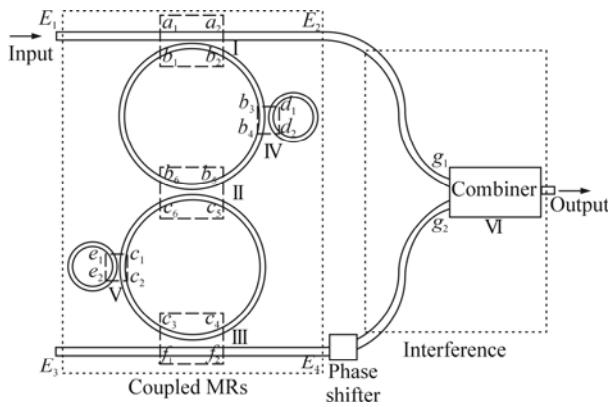

Fig.1 Schematic diagram of the cascaded microring filter with two master rings and two slave rings

There are six coupling sections in this filter. Three of them are between ring and ring, two of them are between ring and bus, and the last one is between two buses. Here,

* This work has been supported by the National Natural Science Foundation of China (No.61172044), and the Natural Science Foundation of Hebei Province (No.F2012203204).
** E-mail:owen88zjnbzhx@126.com

we do not consider the overlapping of these coupling sections, which means the embedded microrings should not be set on the coupling area between bus and big rings.

In this simulation, we use transfer matrix method[16] instead of finite-difference time-domain (FDTD) method. Define the amplitude coupling coefficient as k_i（i=1, 2, 3, 4, 5）and amplitude transmission coefficient as t_j (j=1, 2, 3, 4, 5）in sections I, II, III, IV and V, which obey $t_i^2+t_j^2=1$ under the ideal condition. The transfer matrices of five sections in the left part can be expressed as

$$\begin{bmatrix} b_1 \\ b_2 \end{bmatrix} = \begin{bmatrix} -\frac{t_1}{\mathrm{j}k_1} & \frac{1}{\mathrm{j}k_1} \\ -\frac{1}{\mathrm{j}k_1} & \frac{t_1}{\mathrm{j}k_1} \end{bmatrix} \begin{bmatrix} a_1 \\ a_2 \end{bmatrix}, \tag{1}$$

$$\begin{bmatrix} c_5 \\ c_6 \end{bmatrix} = \begin{bmatrix} -\frac{t_2}{\mathrm{j}k_2} & \frac{1}{\mathrm{j}k_2} \\ -\frac{1}{\mathrm{j}k_2} & \frac{t_2}{\mathrm{j}k_2} \end{bmatrix} \begin{bmatrix} b_5 \\ b_6 \end{bmatrix}, \tag{2}$$

$$\begin{bmatrix} f_1 \\ f_2 \end{bmatrix} = \begin{bmatrix} -\frac{t_3}{\mathrm{j}k_3} & \frac{1}{\mathrm{j}k_3} \\ -\frac{1}{\mathrm{j}k_3} & \frac{t_3}{\mathrm{j}k_3} \end{bmatrix} \begin{bmatrix} c_3 \\ c_4 \end{bmatrix}, \tag{3}$$

$$\begin{bmatrix} d_1 \\ d_2 \end{bmatrix} = \begin{bmatrix} -\frac{t_4}{\mathrm{j}k_4} & \frac{1}{\mathrm{j}k_4} \\ -\frac{1}{\mathrm{j}k_4} & \frac{t_4}{\mathrm{j}k_4} \end{bmatrix} \begin{bmatrix} b_3 \\ b_4 \end{bmatrix}, \tag{4}$$

$$\begin{bmatrix} e_1 \\ e_2 \end{bmatrix} = \begin{bmatrix} -\frac{t_5}{\mathrm{j}k_5} & \frac{1}{\mathrm{j}k_5} \\ -\frac{1}{\mathrm{j}k_5} & \frac{t_5}{\mathrm{j}k_5} \end{bmatrix} \begin{bmatrix} c_1 \\ c_2 \end{bmatrix}. \tag{5}$$

Here, the circumferences of master rings and slave rings are L_m and L_s, respectively. Thus the waveguide length between coupling sections I and IV is $L_\mathrm{m}/4$. $\tau_\mathrm{m}=\exp(-\alpha_\mathrm{m}L_\mathrm{m})$, where τ_m is the circular trip amplitude transmission factor, and α_m is the bend loss coefficient of master rings. Meanwhile, the circular trip phase transmission factor can be expressed as $p_\mathrm{m}=\exp(\mathrm{i}\beta L_\mathrm{m})$. Similarly, the circular trip amplitude and phase transmission factors of slave rings are written as $\tau_\mathrm{s}=\exp(-\alpha_\mathrm{s}L_\mathrm{s})$ and $p_\mathrm{s}=\exp(\mathrm{i}\beta L_\mathrm{s})$, respectively. Then, we have the transmission procedure as

$$b_3 = (\tau_\mathrm{m} p_\mathrm{m})^{\frac{1}{4}} b_2 , \tag{6}$$

$$b_5 = (\tau_\mathrm{m} p_\mathrm{m})^{\frac{1}{4}} b_4 , \tag{7}$$

$$b_1 = (\tau_\mathrm{m} p_\mathrm{m})^{\frac{1}{2}} b_6 , \tag{8}$$

$$d_1 = (\tau_\mathrm{s} p_\mathrm{s}) d_2 , \tag{9}$$

$$c_1 = (\tau_\mathrm{m} p_\mathrm{m})^{\frac{1}{4}} c_6 , \tag{10}$$

$$c_3 = (\tau_\mathrm{m} p_\mathrm{m})^{\frac{1}{4}} c_2 , \tag{11}$$

$$c_5 = (\tau_\mathrm{m} p_\mathrm{m})^{\frac{1}{2}} c_4 , \tag{12}$$

$$e_1 = (\tau_\mathrm{s} p_\mathrm{s}) e_2 . \tag{13}$$

If we pair one master ring and one slave ring as one ring group, according to Eqs.(4)–(13), the transfer matrices of two groups in our structure can be described as

$$\begin{bmatrix} b_5 \\ b_6 \end{bmatrix} = \begin{bmatrix} 0 & (\tau_\mathrm{m} p_\mathrm{m})^{\frac{1}{2}} (t_4 - \frac{k_4^2}{(\tau_\mathrm{s} p_\mathrm{s})^{-1} - t_4}) \\ (\tau_\mathrm{m} p_\mathrm{m})^{-\frac{1}{2}} & 0 \end{bmatrix} \begin{bmatrix} b_1 \\ b_2 \end{bmatrix}, \tag{14}$$

$$\begin{bmatrix} c_3 \\ c_4 \end{bmatrix} = \begin{bmatrix} 0 & (\tau_\mathrm{m} p_\mathrm{m})^{\frac{1}{2}} (t_5 - \frac{k_5^2}{(\tau_\mathrm{s} p_\mathrm{s})^{-1} - t_5}) \\ (\tau_\mathrm{m} p_\mathrm{m})^{-\frac{1}{2}} & 0 \end{bmatrix} \begin{bmatrix} c_5 \\ c_6 \end{bmatrix}. \tag{15}$$

Combining Eqs.(1)–(3), (14) and (15), the transfer formula of whole left part can be deduced as

$$\begin{bmatrix} f_1 \\ f_2 \end{bmatrix} = \begin{bmatrix} -\frac{t_1}{\mathrm{j}k_1} & \frac{1}{\mathrm{j}k_1} \\ -\frac{1}{\mathrm{j}k_1} & \frac{t_1}{\mathrm{j}k_1} \end{bmatrix} \cdot \begin{bmatrix} 0 & (\tau_\mathrm{m} p_\mathrm{m})^{\frac{1}{2}} (t_4 - \frac{k_4^2}{(\tau_\mathrm{s} p_\mathrm{s})^{-1} - t_4}) \\ (\tau_\mathrm{m} p_\mathrm{m})^{-\frac{1}{2}} & 0 \end{bmatrix} \begin{bmatrix} -\frac{t_2}{\mathrm{j}k_2} & \frac{1}{\mathrm{j}k_2} \\ -\frac{1}{\mathrm{j}k_2} & \frac{t_2}{\mathrm{j}k_2} \end{bmatrix} \cdot \begin{bmatrix} 0 & (\tau_\mathrm{m} p_\mathrm{m})^{\frac{1}{2}} (t_5 - \frac{k_5^2}{(\tau_\mathrm{s} p_\mathrm{s})^{-1} - t_5}) \\ (\tau_\mathrm{m} p_\mathrm{m})^{-\frac{1}{2}} & 0 \end{bmatrix} \cdot \begin{bmatrix} -\frac{t_3}{\mathrm{j}k_3} & \frac{1}{\mathrm{j}k_3} \\ -\frac{1}{\mathrm{j}k_3} & \frac{t_3}{\mathrm{j}k_3} \end{bmatrix} \begin{bmatrix} a_1 \\ a_2 \end{bmatrix}. \tag{16}$$

Eq.(16) is denoted as $\begin{bmatrix} f_1 \\ f_2 \end{bmatrix} = \boldsymbol{M} \begin{bmatrix} a_1 \\ a_2 \end{bmatrix}$, where $\boldsymbol{M}$ is the transfer matrix calculated before, i.e., $\boldsymbol{M} = \begin{bmatrix} m_{11} & m_{12} \\ m_{21} & m_{22} \end{bmatrix}$.

If the loss in straight waveguide is not considered, the intensities of E_2 and E_4 are given as

$$\left| \frac{E_2}{E_1} \right|^2 = \left| -\frac{m_{11}}{m_{12}} \right|^2 , \tag{17}$$

$$\left| \frac{E_4}{E_1} \right|^2 = \left| -\frac{\mathrm{Det}(\boldsymbol{M})}{m_{12}} \right|^2 . \tag{18}$$

In the Y junction, the output normalized intensity of the whole system can be expressed as

$$I_{\text{out}}=\left|\frac{E_{\text{out}}}{E_{1}}\right|^{2}=\left|-\frac{m_{11}}{m_{12}}-\frac{\text{Det}(\boldsymbol{M})}{m_{12}}\right|^{2} . \tag{19}$$

Based on the theory deduced above, the spectral responses at filter output port are simulated by Matlab. Since the value of coupling coefficient can significantly influence the spectral form, the proper choices of coupling coefficients can markedly improve the filter performance. We divide the left five coupling sections into the section between bus and mater ring, the section between master rings and the section between master ring and slave ring. Assume that the coupling sections in the same group have the same coupling coefficient, namely $k_1=k_3=k_{\mathrm{I}}$, $k_4=k_5=k_{\mathrm{III}}$ and $k_2=k_{\mathrm{II}}$.

Extinction ratio and full width at half maximum (FWHM) should be major factors to be concerned during the choice of coupling coefficient. The higher ratio means the better filter effect, which also means high sensing efficiency in amplitude detection sensor design. The lower FWHM means higher Q-factor and higher transmission. For the sensors which covert signal to the shift of resonant wavelength[17], it also means higher precision of the sensor.

After several numerical tests, we choose k_{I}=0.3, k_{II}=0.02 and k_{III}=0.06 as the coupling coefficients of three kinds of sections. Keeping two coupling coefficients as constant, the relationship between the other coupling coefficient and extinction ratio is shown in Fig.2. When k_{I} is around 0.3, the extinction ration is more than 20 dB. Similarly, the extinction ratio reaches the bottom when k_{III} is nearly 0.06. According to Fig.2(b), the extinction effect is very obvious in low value of k_{II}. Considering the transmission, we choose k_{II}=0.02 to keep the extinction ratio more than 20 dB. From Fig.2, we know these three values of coupling coefficients mentioned above can keep the extinction ratio more than 20 dB.

FWHM also depends on the values of coupling coefficients. Fig.3 shows the main modes at resonant wavelength, whose FWHMs change obviously with the decrease of coupling coefficients in each section.

As shown in Fig.3(a), the main mode becomes narrower with the decrease of k_{I}, while Q-factor becomes higher. The relationship between k_{III} and FWHM has the similar trend as shown in Fig.3(c). For k_{II}, the peaks become a unity with the decrease of k_{II}. According to Fig.3(b), when k_{II} is 0.6 and 0.2, the main mode evidently splits in two resonant peaks. Even though k_{II}=0.08, the peaks are still not united. The main mode does not become one resonant peak until k_{II} decreases to 0.02. Based on the numerical simulation of coupling coefficient above, it is easy to conclude that the three coefficients we choose are proper for the structure which pursues larger extinction ratio and higher Q-factor.

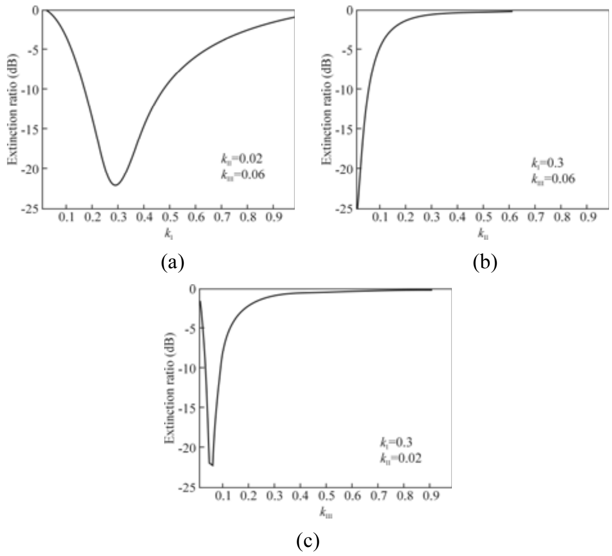

Fig.2 Relationship between coupling coefficients and extinction ratio

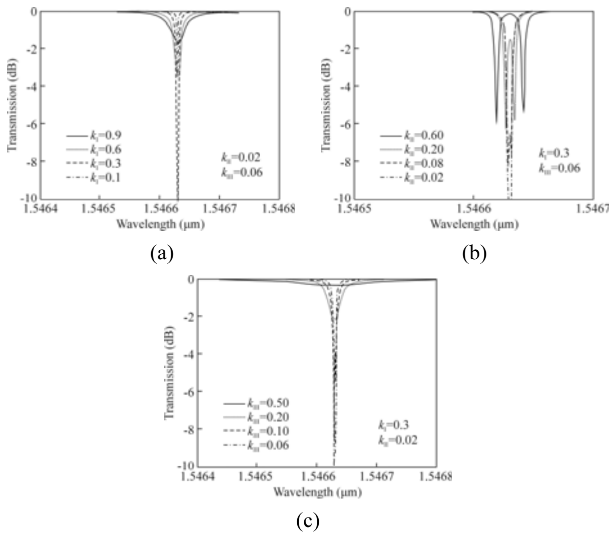

Fig.3 Output spectra of the structures with different coupling coefficients at resonant wavelength

The output spectrum of this filter is shown in Fig.4(a). For the structure with two cascaded master rings and two slave rings, the extremely wide FSR of 206 nm and the extinction ratio of 24 dB at resonant wavelength are obtained. From Fig.4(a), spurious mode is hardly to be found. If we magnify the graph, which is shown in Fig.4(b), the spurious mode can be found but is extremely suppressed by the structure we designed. The largest extinction ratio of spurious mode is no more than 0.1 dB. It means that these spurious modes can be ignored.

Although the proposed structure is not as simple as some filters reported before[2,14-16], every part is necessary to obtain such an excellent output spectrum with extremely large FSR, high extinction ratio and narrow bandwidth. Now we use comparisons to prove the necessity of each part. First of all,

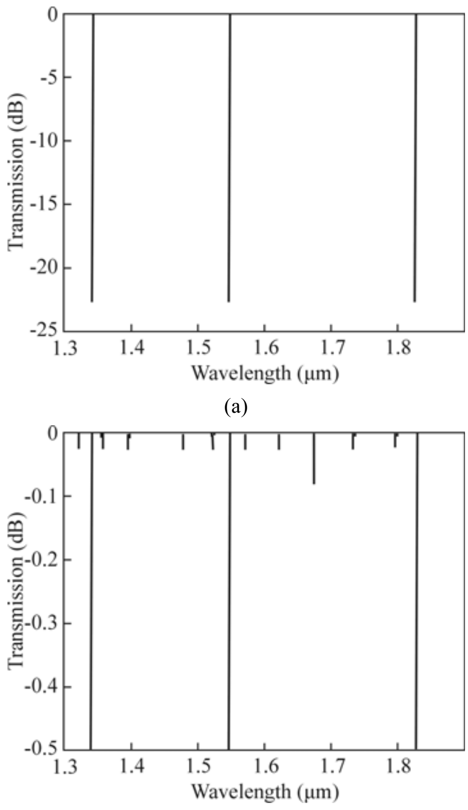

(a)

(b)

Fig.4 (a) Output spectrum and (b) magnified output spectrum of the designed compact filter

change the cascaded number, namely the number of ring groups. The similar structure with only one master ring and one slave ring and its output spectrum are depicted in Fig.5. For this structure, the extinction ratio is only about 5 dB, which is much lower than that of our structure. It means adding another ring group can significantly improve the filter effect by enlarging the extinction ratio. Secondly, compare our structure with the structures without slave rings shown in Fig.6(a). It is well-known that adding slave rings can expand FSR because of Vernier effect[18]. From Fig.6(b), the output spectrum of filter without slave rings shows that the extinction ratio is only 0.02 dB, and FSR is 40 nm, which proves that adding slave rings is necessary for optimizing the filter effect. Thirdly, verify the effects of combiner and phase shifter on suppressing the spurious modes generated from cascaded structure. If we remove the combiner and the phase shifter and only detect the spectral response from the top bus, the output spectra of structures with one ring group and cascaded two ring groups are shown in Fig.7(a) and (b), respectively. For the structure only with one master ring and one slave ring, the extinction ratio of spurious mode is more than 20 dB, and the FSR is also small. Meanwhile, for the structure with two cascaded ring groups, although the FSR is expanded to about 200 nm, the extinction ratio of the spurious mode is still 7 dB. If we add a combiner and a phase shifter as the structure we proposed, the spurious mode is suppressed to less than 0.1 dB as shown in Fig.4. To sum up, the two cascaded master rings can enlarge the extinction ratio of main modes, and the slave rings coupled with master rings can expand the FSR, so the combiner and phase shifter can extremely suppress the spurious modes. Therefore, these three parts are all necessary for the optimization of output spectrum of the filter for sensor application.

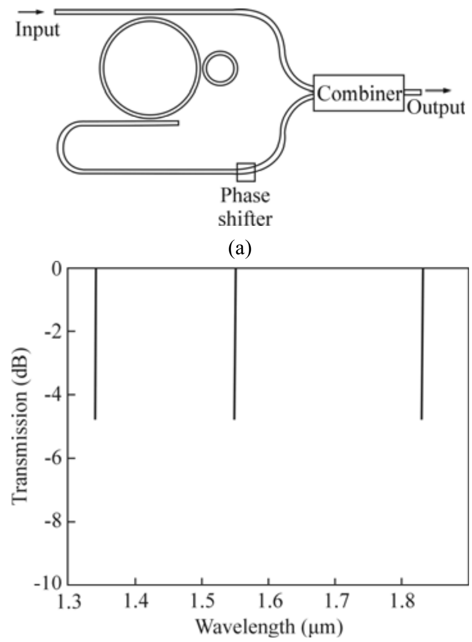

(a)

(b)

Fig.5 (a) Structure without cascaded ring group and (b) its output spectrum

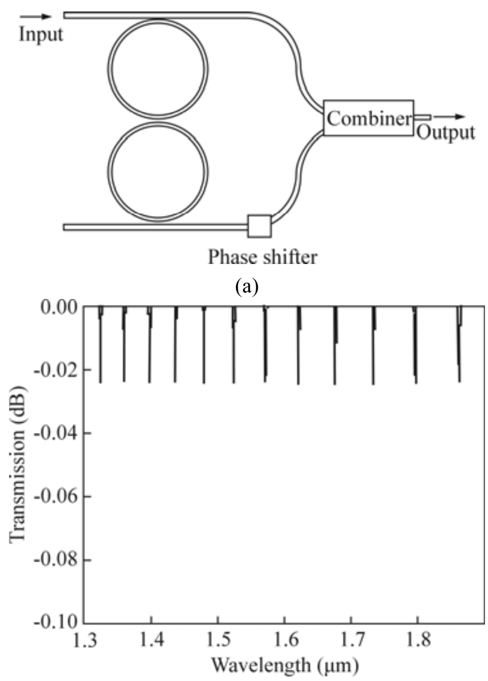

(a)

(b)

Fig.6 (a) Structure without slave rings and (b) its output spectrum

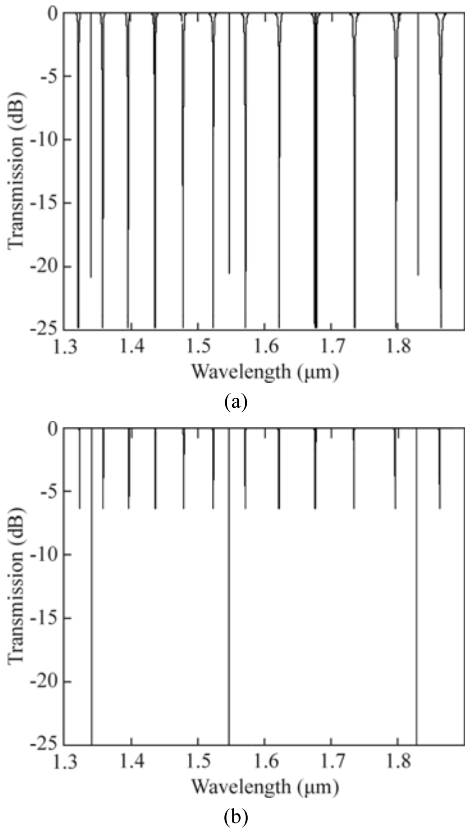

Fig.7 Output spectra of structures with (a) one ring group and (b) cascaded two ring groups without combiner and phase shifter

An ultra-compact microring filter consisting of two master rings with radius of 2.5 μm and two slave rings with radius of 1 μm is demonstrated. According to the theoretical simulation, Q-factor and FSR can reach 2.76×10^5 and 206 nm, respectively. Meanwhile, it can keep the extinction ratio of main mode more than 25 dB and suppress the spurious mode to less than 0.1 dB, which shows excellent performance as a narrow band filter. Based on the simple single ring structure reported before, our design optimizes the filter effect by two ways. One is adding cascaded master ring, slave rings and combiner to enlarge the extinction ratio of main modes, expand the FSR and suppress the spurious mode generated by adding rings. The other one is to choose proper coupling coefficient in each coupling section, which ensures high Q-factor and obvious extinction of main modes. The results show that the filter we designed can achieve very good performance as a filter for sensor application.

References

[1] Hongwei Jiang and Yuanda Wu, Journal of Optoelectronics·Laser **22**, 813 (2011). (in Chinese)

[2] Wei Wang, Aihua Zhang, Keng Yang, Zhan Huang, Feng shijuan and Yuesheng Wang, Ultracompact SOI Microring Add Drop Filter with Extra-Wide FSR for Silicon Photonic Application, Symposium on Photonics and Optoelectronics, 1 (2012).

[3] Zhuoni Fan, BinFeng Yun, Guohua Hu, Yijian Yan and Yiping Cui, Journal of Optoelectronics·Laser **23**, 1727 (2012). (in Chinese)

[4] P. Dong, R. Shafiiha, S. Liao, H. Liang, N.-N. Feng, G. Li and X. Zheng, Optics Express **18**, 10941 (2010).

[5] Jianxiong Tang, Yaohui Jin, Zhijuan Chang, Xiaming Chen and Tong Ye, Opt. Eng. **50**, 094002 (2011).

[6] Lin Yang, Ruiqiang Ji, Lei Zhang, Jianfeng Ding and Qianfan Xu, Optics Express **20**, 13560 (2012).

[7] Matthew S. Luchansky and Ryan C. Bailey, Analytical Chemistry **84**, 793 (2012).

[8] Rozalia Orghci, Peter Lützow, Jörg Burgmeier, Jan Koch, Helmut Heidrich, Wolfgang Schade, Nina Welschoff and Siegfried Waldvogel, Sensors **10**, 6788 (2010).

[9] Huaxiang Yi, David S. Citrin and Zhiping Zhou, IEEE Journal of Quantum Electronics **47**, 354 (2011).

[10] W. Bogaerts, P. De Heyn, T. Van Vaerenbergh, K. De Vos, S. Kumar Selvaraja, T. Claes, P. Dumon, P. Bienstman, D. Van Thourhout and R. Baets, Laser Photonics Reviews **6**, 47 (2012).

[11] Jianwei Wang, Sailing He and Daoxin Dai, Silicon-nanowire-based Optical Sensor by using Mach-Zehnder Interferometer Coupled Microring, Asia Communications and Photonics Conference and Exhibition, 322 (2010).

[12] Daoxin Dai and Sailing He, J. Opt. Soc. Am. B **26**, 511 (2009).

[13] Qianfan Xu, David Fattal and Raymond G. Beausoleil, Optics Express **16**, 4309 (2008).

[14] Junbo Feng, Qunqing Li and Zhiping Zhou, IEEE Photonics Technology Letters **23**, 79 (2011).

[15] Ying Lu, Xiangyong Fu, Danping Chu, Wuqi Wen and Jianquan Yao, Optics Communications **284**, 476 (2011).

[16] Nebiyu A.Yebo, Petra Lommens, Zeger Hens and Roel Baets, Optics Express **18**, 11859 (2010).

[17] Enming Xu, Xinliang Zhang, Lina Zhou, Yu Zhang, Yuan Yu, Xiang Li and Dexiu Huang, Optics Letters **35**, 1242 (2010).